CIVIL ENGINEERING JOURNAL

Article no. 59

THE CIVIL ENGINEERING JOURNAL 3-2021

GEOPHYSICAL SURVEY AS A TOOL TO REVEAL SUBSURFACE STRATIFICATION AT WITHIN A SMALL AGRICULTURAL HEADWATER CATCHMENT: A CASE STUDY

Jakub Jeřábek and David Zumr

Czech Technical University in Prague, Faculty of Civil Engineering, The Department of Landscape Water Conservation, Prague, Thákurova 7/2077, 166 29, Praha 6 - Dejvice, Czech Republic; e-mail: jakub.jerabek@fsv.cvut.cz

ABSTRACT

Managers use the catchment as a basic spatial unit in landscape hydrology to estimate local water balance and manage water resources. The catchment drainage area is commonly delineated based on the surface topography, which is determined using a digital elevation model. Therefore, the surface outflow only is implicitly considered. However, a substantial portion of the rainfall water infiltrates and percolates through the soil profile towards the groundwater, where geological structures control the drainage area instead of the soil surface topography. The discrepancy between the surface topography-based and bedrock-based drainage area can cause larger discrepancies in water balance calculations. It this paper, we present the investigation of the subsurface media stratification within the headwater catchment, located in the central part of the Czech Republic using a geophysical survey method - electrical resistivity tomography (ERT). Results indicate that the complexity of the subsurface geological layers cannot be estimated solely from the land surface topography. Although the shallow layers follow the shape of the surface, the deeper layers do not. This finding has a strong implication on the water flow regime since it suggests that the deep drainage may follow different pathways and other preferential directions as compared to the water flow within the shallow subsurface.

KEYWORDS

Electrical resistivity tomography, Hydrology, Subsurface stratigraphy, Headwater catchment

INTRODUCTION

Catchment drainage area is a key concept in hydrology. It is defined by the catchment topographical boundaries which restrict the area from which all of the water flows to the common outlet. The catchment divide serves as a delineation between the adjacent catchments. Catchment drainage area also serves as a representative unit for water balance calculation. Water management is usually catchment-based as it is difficult to administrate the water resources within the landscape with politically designed boundaries where the water balance is not closed. The orographic divide is commonly used to delineate the catchment area. It is derived by means of topography (i.e. on a digital elevation model), therefore it is typically located at the ridge or a hilltop as is shown in Figure 1a. In some cases, the hydrogeological setting in the subsurface creates a low permeable geological layer in a way that the water which infiltrates towards this layer flows in opposite direction compared to the overlaying soil surface (Figure 1b). Knowledge about the subsurface stratification is important in order to be able to close or complete the water balance equation, since the water flow through the catchment orographic boundary may be affected by those layers [1]. However, the information about the subsurface settings at a catchment is not always available.

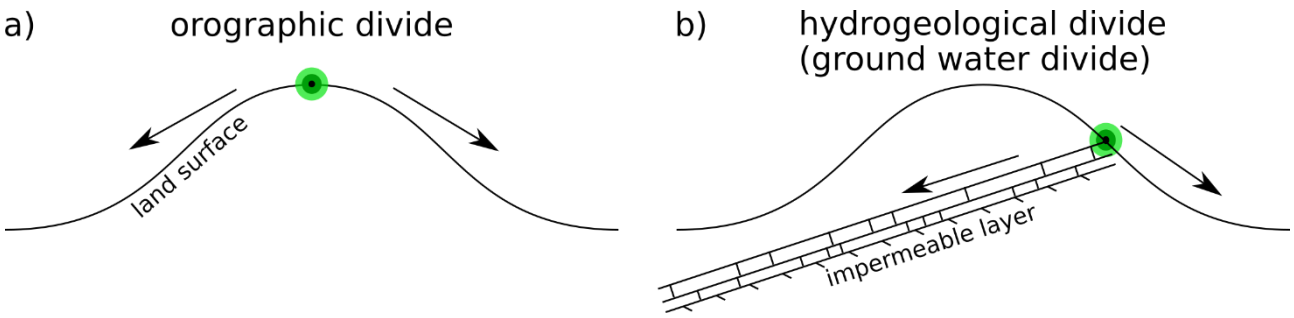

Fig. 1 – Difference between a) orographic and b) hydrogeological divide. Arrows indicate direction of the flowing water. Green dots indicate the divide.

Geophysical survey is a common option how to investigate the subsurface structures and the bedrock position. Number of geophysical techniques are available for practice and research purposes. The most common ones are: ground penetration radar, seismic refraction, magnetic methods, and electrical resistivity tomography [2]. Ground penetration radar (GPR), emits and detects electromagnetic pulses. The pulses are reflected from contrasted dialectical properties. Although GPR provides the best spatial resolution, it is not a suitable technique for materials with low contrast dielectric properties and in general for materials with lower el. resistivity than ca. 50 – 100 Ωm [2]. Seismic reflection uses geophones to detect a velocity of seismic waves introduced with sledgehammer (or earthquake). Although this method is well suited for bedrock detection and can reach deeper depths, it requires an increasing density of subsurface layers with depth. Magnetic methods are based on measuring of the magnetic properties (magnetic susceptibility) which reflect upon different concentrations of various ferromagnetic materials in the subsurface. Electrical resistivity tomography has shown to be a promising tool for its versatility and ease to obtain the field data. The depth ranges and spatial resolution can be easily set by the user. However, the technique requires good connection between the material and electrodes (principle explained bellow) and does not provide good results within a blocky subsurface structure [2].

In this study, we utilize the electrical resistivity tomography method (ERT), as described e.g. by Samouëlian et al. [3]. In principle, ERT can be used to detect the spatial distribution of electrical resistivity in the subsurface by introducing electrical current to the soil and detecting the resulting voltage of the subsurface media (more details are provided in the Methods section). Distinct soil layers or various rock materials, as well as soils of various water saturation, have different electrical resistivity [3], and therefore different subsurface structures can be detected and delineated.

ERT has been widely used in many fields of research and practical applications in various spatial scales, such as investigation of landslide to design protection measures (e.g. [4]), identification and delineation of soil contamination e.g. [5], [6], investigation of leachate from a landfill [7] or mixing of fresh and seawater in the coastal areas [8], [9]. ERT has been used to delineate individual soil layers above the bedrock [10] or even to study the shallow part of the soil profile (topsoil) where the tillage takes place [11], [12], and it is also commonly used in archaeology [13]. Furthermore, ERT has also been successfully used to identify the bedrock position in karst areas, where the heterogeneous bedrock (caused by uneven dissolution of the limestone) makes such a task very challenging [14], [15]. The representatives of the ERT method was successfully evaluated when compared with soil layers stratification observed in excavated trenches [14].

In this study we utilize electrical resistivity tomography (ERT) to observe and delineate subsurface structures and the bedrock, within a small agricultural headwater catchment. The main objective is to improve the understanding of the geological layering at the catchment in order to be able to assess movement of water e.g. via hydrological models [16].

METHODS

Study area

The study was performed at the experimental catchment Nučice which is located at the central part of the Czech Republic (Figure 2). The catchment area is 53 ha with a mean slope of 3.9%. The majority of the catchment is covered with arable land (96.4%). The soils are classified as Cambisols and Haplic Luvisols with sandy loam texture. The bedrock consists of layers of sandstone, siltstone and conglomerate from Carboniferous and Permian geological period (geological map CR, Figure 2). The Czech Geological Survey classifies the whole catchment area as "Alternating sandstone and claystone – permeability low to moderate". For more information about the catchment and instrumentation at the catchment we refer to [17].

The deep ground water level was observed at 355 m a.s.l. (57.7 m below ground surface) within a nearby borehole survey. The borehole survey was performed in the southern direction at a distance of 700 meters (m) from the west-south edge of the catchment. The borehole survey showed sandstone and conglomerate layers with thickness up to 10 meters.

The shallow groundwater level (GWL) of the quaternary alluvial aquifer was measured at two locations in the catchment (Figure 2). Generally, the shallow GWL dropped 3 m below the soil surface during prolonged dry periods in the summer. During heavy rain events GWL almost reached the surface. For most of the year the groundwater is between 2 and 3 m below the ground. The shallow and deep groundwater indicate a complex hydrogeological situation within the catchment, where the proposed ERT survey may help to understand the system.

There are 3 separated fields at the catchment: the top field (Figure 2) and bottom fields (fields 2 and 3 in Figure 2). The asphalt road separates the top and bottom fields. An ephemeral stream is located between the fields 2 and 3. The stream starts at the lowest part of the top field where outlet from tile drain is located. The tile drain then continues in thalweg to the other side of the field 1 where the main road is located near the catchment boundary.

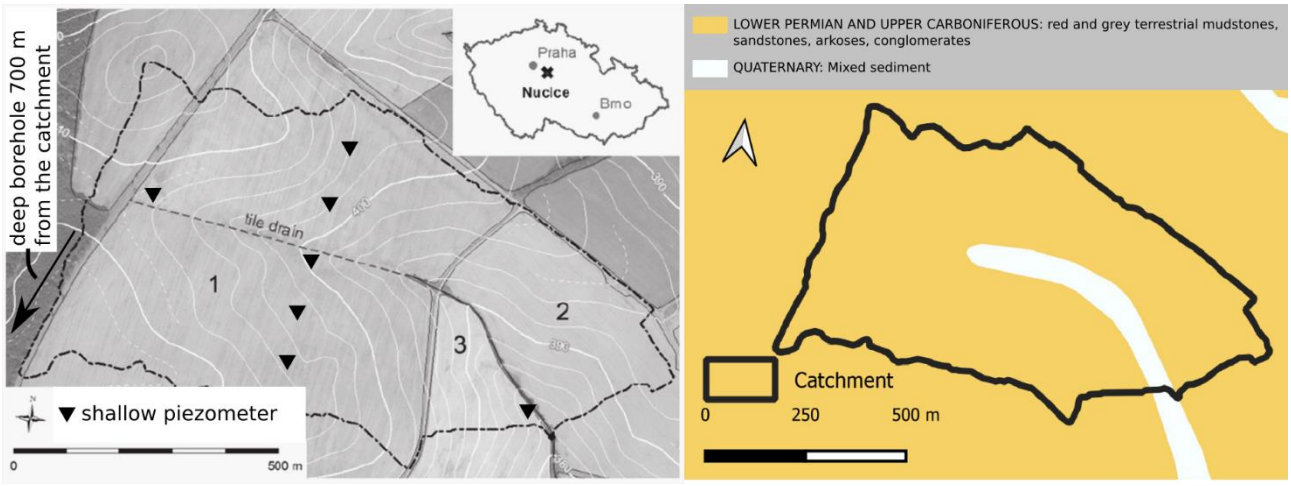

Fig. 2 - .The experimental catchment (left). The numbers stand for three different fields. Location of the shallow groundwater level monitoring and the location of borehole are indicated in the map. Geological map of the experimental catchment (right) © ČGS.

Soils and rocks of different composition and water saturation have distinct electrical properties. The electrical resistivity of the shallow soil layers (down to 1 meter from the surface) was measured at the same catchment by Jerabek et al. [11], the values ranged between 20 – 50 Ωm. The electrical resistivity of the sedimentary rocks is usually considerably higher, the literature reports values in a wide range of 10 – 10^4 Ωm order of magnitude [18], [19]. According to [20] the electrical resistivity of relevant media is shown in Table 1.

Tab. 1: overview of materials and their electrical resistivity (based on [20])

		electrical resistivity Ωm	
origin	material	from	to
shield un-weathered rocks	massive sulfides, graphite	0.01	10
	Igneous and metamorphic rocks	1000	100000
weathered layered		1	10000
glacial sediments	clays	3	100
	tills	30	3000
	gravel and sand	30	10000
sedimentary rocks	shales	50	300
	sandstone and conglomerate	50	10000
	lignite, coal	10	700
	dolomite, limestone	1000	100000
water, aquifers	salt water	0.3	1
	fresh water	2	100

Electrical resistivity tomography

The electrical resistivity tomography (ERT) survey consists of several steps. The so-called apparent electrical resistivity data is collected in the field. In this step, a number of electrodes are inserted into the soil surface along the line (in the case of a 2D profiling). An electrical field is introduced by a pair of electrodes (current electrodes) in the soil, while another pair of electrodes (potential electrodes) measures the voltage caused by the electrical field in the subsurface structure. Configuration of current and potential (voltage) electrodes, commonly called ERT array, exhibits varying horizontal or vertical spatial resolution, and sensitivity to the vertical (e.g. buried boulders) or horizontal (e.g. soil horizons or groundwater level) structures [3, 21]. Based on the geometry of the ERT array a hemisphere with a given apparent electrical resistivity is constructed.

The apparent electrical resistivity data collected has to be processed by inverse numerical modelling in order to obtain real electrical resistivity at a given location in the measured transect [22]. In the inversion procedure, the electrical resistivity is optimized based on the given ERT array and the apparent electrical resistivity data. In some cases, thousands of values need to be optimized which makes the process nontrivial and computationally intensive [22]. The numerical inversion also introduces a certain degree of uncertainty in the results and has to be considered during the data interpretation.

ERT survey design

Five independent ERT transects were performed within this study. An overview of the measured transects is shown in Table 2. Each of the ERT profiles consisted of several individual overlapping sub-transects which were merged before inversion. Most of the measurements were performed with the electrode spacing of 5 m, except the measurements BFC3 and TFC3 with 3 m electrode spacing. Location and orientation of each transect is shown in Figure 3. Two transects follow the thalweg and brook of the catchment, three transects cross the catchment perpendicularly to the catchment thalweg and the stream (Figure 3). There were three interceptions of the ERT transects; two in the field 1 and one in bottom fields 2 and 3.

Tab. 2: Overview of all measured ERT transects.

Date mm/yyyy	Measurement ID	Transect length [m]	Electrode spacing [m]	Location at the catchment – orientation
04/2012	BFC3	540	3	Bottom fields – cross
12/2016	TFC3	444	3	Top field – cross
08/2019	BFB5	395	5	Bottom fields – brook
10/2019	TFC5	620	5	Top field – cross
10/2019	TFT5	580	5	Top field – thalweg

Automatic resistivity system (ARES, GF Instruments, Brno, Czech Republic) was used to obtain the apparent resistivity data. Wenner-Schlumberger array was used for all the measurements. Res2DInv software was used for the data inversion to calculate the electrical resistivity profiles [22]. Total of 1233 (in case of BFB5) to 3161 (in case of BFC3) data points were inverted with the Res2DInv. The software reached the values of the absolute error between the measured end inverted data below 1.5% after 5 – 6 iterations. The robust inversion method (which is more suitable for layers detection) was used for all transects. The topography of each transect was extracted from the digital elevation model with 1 m spatial resolution.

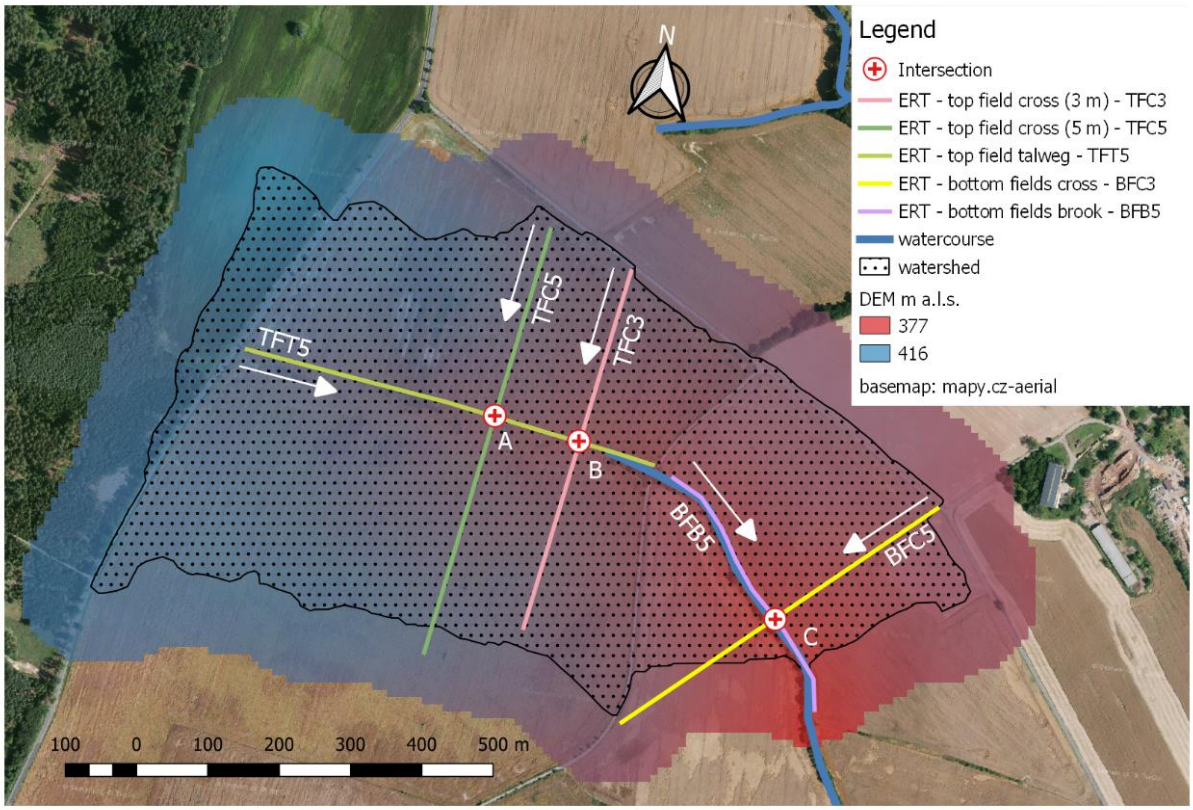

Fig. 3 - The location and intersections of the measured transects. Arrows indicate start and direction of each transect. Digital elevation model provided (C) ČÚZK.

RESULTS

ERT transects

All ERT profiles show electrical resistivity (ρ) in a range of 20 – 150 Ωm. The highest ρ was observed either in the layer located 4 to 6 m below the soil surface or in the deeper layer which is located 15 to 20 m below the soil surface. Soil layer of lower ρ (30 to 50 Ωm) is found in between these regions. Such a layering is clearly visible in the field 1 on transects TFT5, TFC5 and TFC3. Although the same pattern was observed in the bottom fields (field 2 and 3; transects BFB5 and BFC3) the alteration with the regions of different resistivity is less clear. Low electrical resistivity was also observed close to the surface in some cases. The resistivity variability of the upper soil layers (only few meters of a depth) could be attributed to varying soil properties which may differ in organic matter and clay content, and in the actual soil moisture conditions.

The thalweg (TFT5) and along-the-brook (BFB5) transects are both shown in Figure 4. Several spots with high electrical resistivity (ρ) are aligned in the depth of approximately 4 to 10 m. The bottom half of the profile also exhibits higher ρ at the transect TFT5. The area with high ρ was also observed within the BFB5 transect, which appears closer to the soil surface.

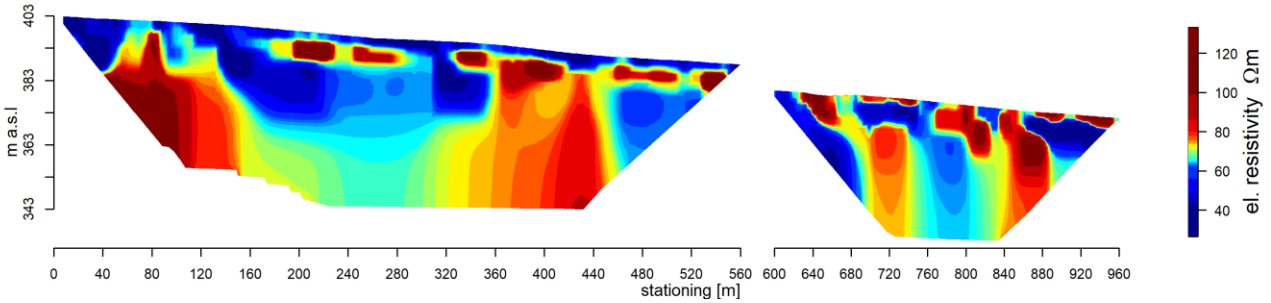

Fig. 4 – ERT transects TFT5 and BTB5 shown in single plot with elevation and stationing starting at the western boundary of the catchment.

The field 1 ERT transects were oriented in the orthogonal direction to the thalweg (TFC transects) and are as shown in Figure 5. Both transects exhibit lower electrical resistivity ρ near the soil surface. High ρ zone near the soil surface areas are restricted only to a limited part of both the transects. Both profiles also exhibit low ρ (below 50 Ωm) in the upper half of each transect. The bottom half of both these transects exhibited higher ρ. Both transects also exhibited the same pattern of the low and high ρ layers despite the different electrode spacing.

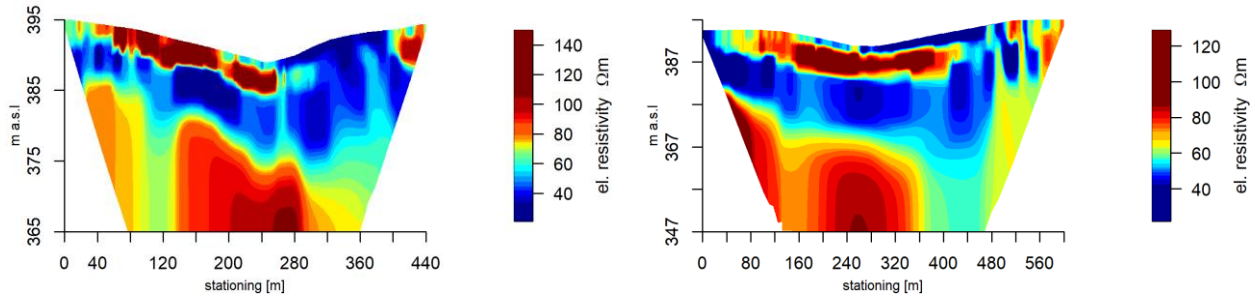

Fig. 5 – ERT transects TFC3 (left) and TFC5 (right).

The ERT profile in the orthogonal direction to the brook (BFC3) transecting the lower fields 2 and 3 is shown in Figure 6. The bottom of the valley is at the stationing of 260 m. The lower ρ was measured only in the shallow part of the field 2 (right hillslope in Figure 6). Below the field 3 (left hillslope in Figure 6) the low ρ layer reaches the depth of approximately 20 m below the soil surface.

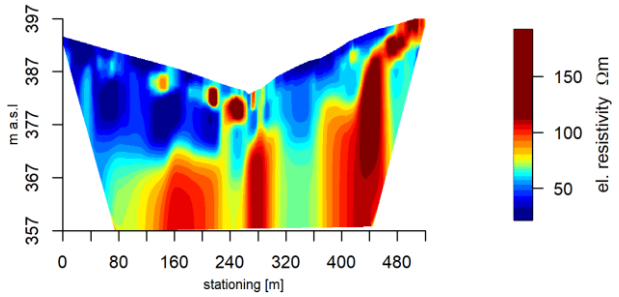

Fig. 6 – BFC3 ERT transects.

ERT transects intersections

The ERT transects were intersected at 3 locations (Figure 7). Intersections A and B were located in the field 1, the intersection C in the field 2 close to the valley. 1D graphs of electrical resistivity ρ with corresponding depth for the 3 intersections are shown in Figure 7. The intersection of transects TFT5 and TFC5 is shown in Figure 7 intersection A. The high ρ values near the soil surface are recognizable in the same depth at both the transects. Also, the second increase of ρ values which can be observed at an altitude of 375 m a.s.l. appeared at a similar depth. The ρ to depth graph of the intersection B (TFT5 and TFC3 ERT transects) exhibited difference in the onset of the shallower high ρ region (Figure 7 intersection B). The difference of the onset was about 2.5 m. The high ρ area which can be observed in the TFC3 profile at an altitude 370 m a.s.l. (approximately 15 m deep) did not appear in the TFT5 transects. Similar results were observed in the intersection of transects BFB5 and BFC3, where onset of the high ρ in near soil surface were also shifted (Figure 7 intersection C). The BFB5 transect exhibited oscillation of the electrical resistivity which could be caused by an error in the measurement or created as an artifact during the mathematical inversion.

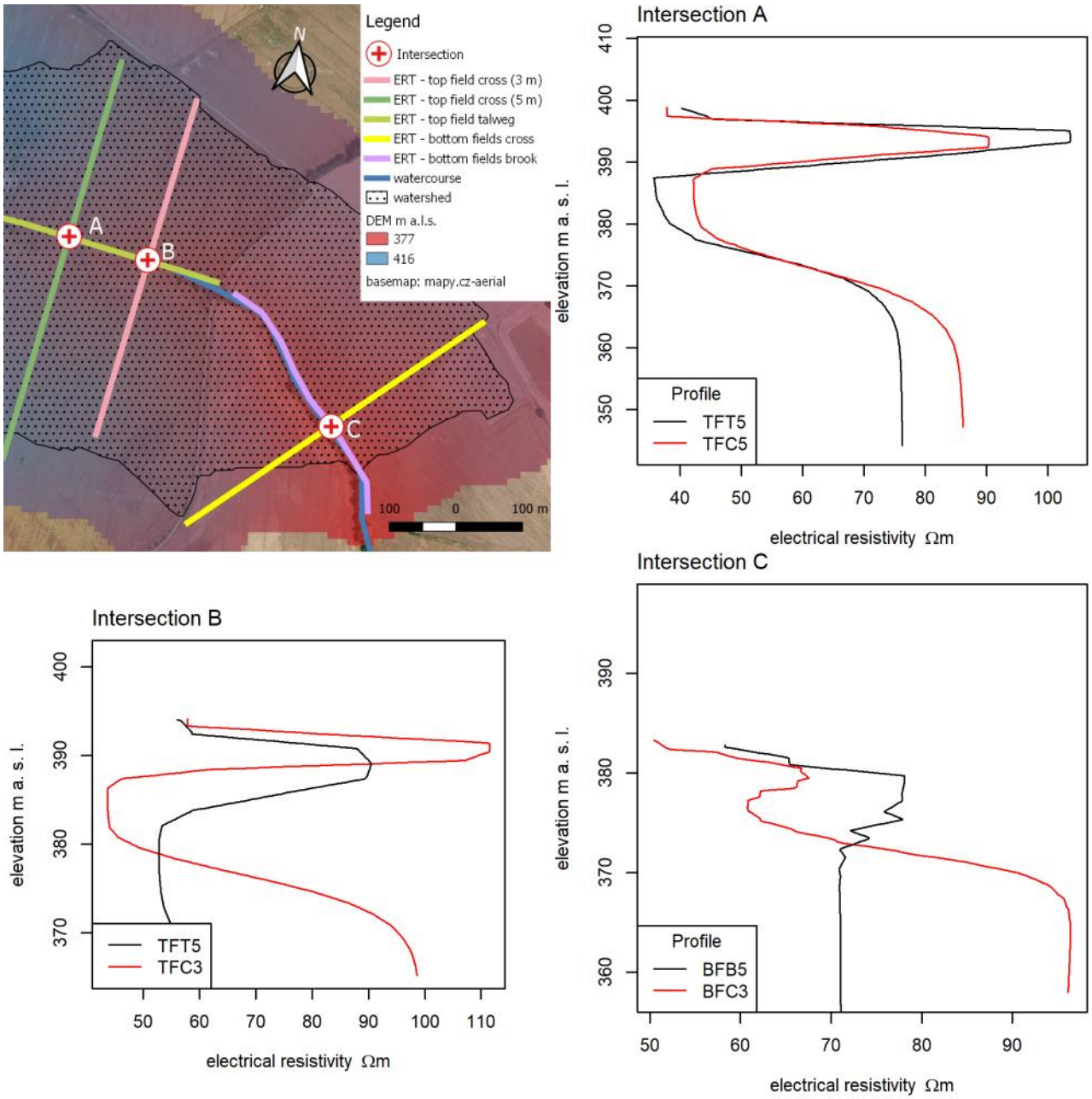

Fig. 7 – Map of intersections and comparison of ERT intersections: intersection A of transects TFT5 and TFC5, intersection B of transects TFT5 and TFC3, and intersection C of transects BFB5 and BFC3.

Hydraulic conductivity of the subsurface structures

Electrical resistivity transects were recalculated with the use of Archie's law [23] to hydraulic conductivity for investigating the hydrological behavior of the subsurface (Figure 8). A high conductive layer is presented at the transects TFC5 and TFC3 overlaid with multiple orders of magnitude lesser conductive layer, probably an aquitard. Presence of a confined aquifer can be hypothesized in this high conductive layer. However, no clear aquitards or aquifers are visible at the perpendicular transects TFT5 and BFB5 or the transect BFC5 at the bottom field. Shallow ground water levels (1 – 3 meter depth) which were recorded in the piezometers indicate an unconfined aquifer on the top of the low-conductivity layer which is visible few meters below the surface. The usage of Archie's law in this context has to be considered only as qualitative metrics, since we cannot

distinguish amongst the various factors affecting the electrical resistivity changes (e.g. soil water content).

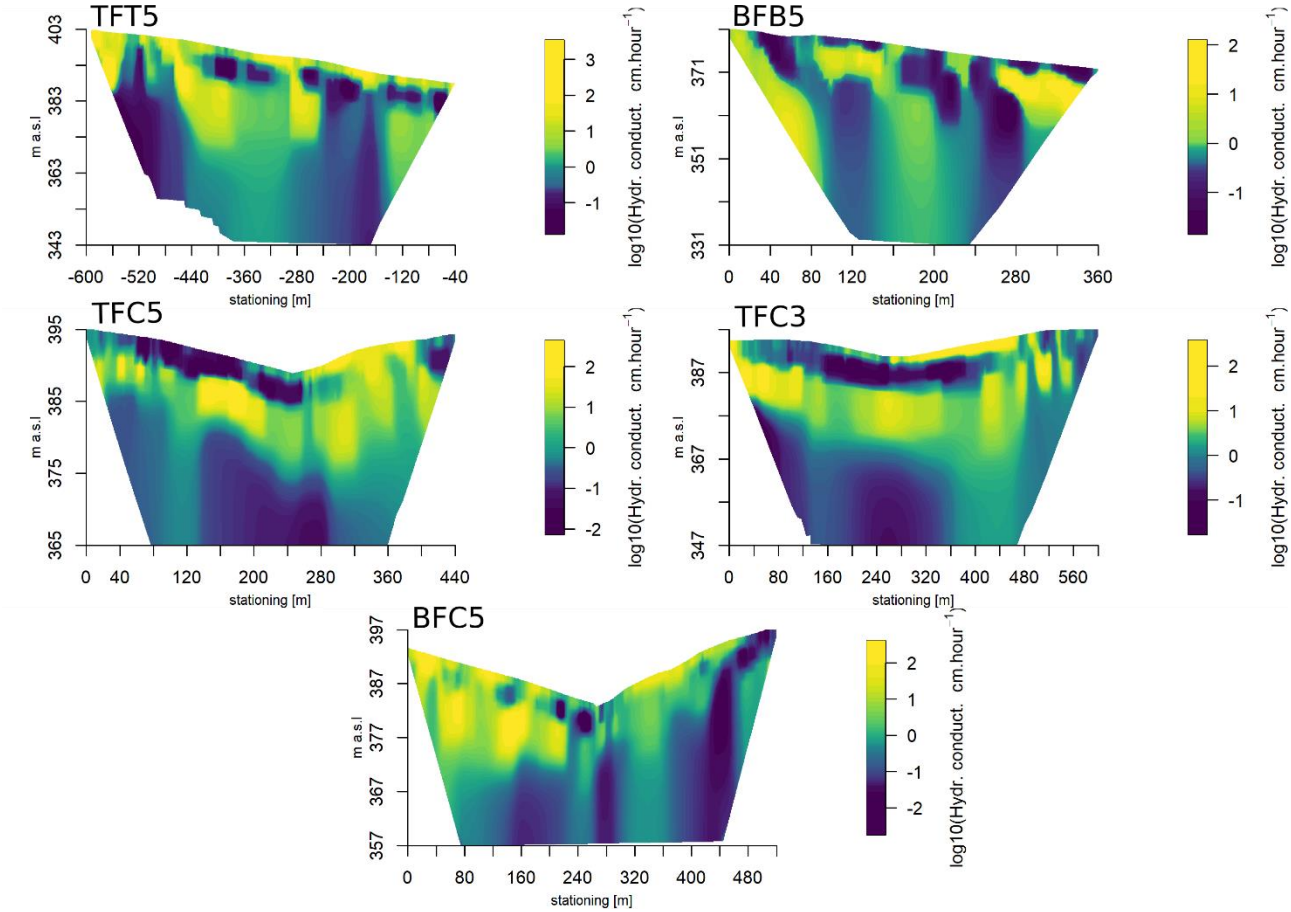

Fig. 8 -The hydraulic conductivity calculated with Archie's law for all the ERT transects.

DISCUSSION

ERT transects

Four distinct layers were distinguished in all ERT transects based on the electrical resistivity values. The layers are shown in Figure 9 (profile TFC5 is shown for illustration):

Layer L1: Low electrical resistivity (ρ) values up to 60 Ω m. Close to the surface - down to the depth of 1 – 2 meters. This layer is not continuous in some transects.

Layer H1: Higher ρ layer. All the transects exhibited areas of higher ρ (up to 150 Ω m) which are located below the layer L1 and reaches the depth of 5 – 10 meters below the soil surface. This layer is more developed at the field 1 compared to fields 2 and 3.

Layer L2: Low ρ layer. This layer exhibit varying thickness and ρ around 40 Ω m. The layer reaches depths down to 25 m below the soil surface.

Layer H2: The bottom of the measured profiles are formed by an area with higher ρ of values above 60 Ω m. Layer H2 is however very heterogeneous, locally reaching resistivity values above 150 Ω m at some transects. It also has to be noted that the ERT profiles exhibit a high degree of uncertainty and lower resolution in the deeper regions.

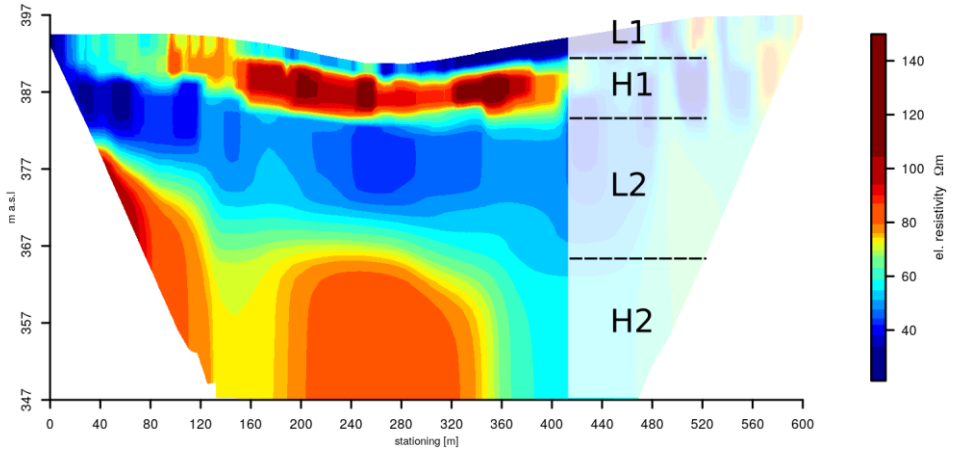

Fig. 9 - The profile TFC5 with clearly developed 4 distinct subsurface layers. Similar stratification is to some extend visible at all measured ERT transects. The TFC5 transect is used here as an example.

The layer L1 is not present in all transects as it is shown in Figure 10. However, in Jeřábek et al. [11], it was shown that the top 1 – 2 meters consist of soil material with ρ around 40 Ωm. The fact that the low ρ layer is not present in all profiles could also be caused by uncertainty in the measured resistivity closer to the surface. The median depth of investigation starts at 2.5 m and 1.55 m for the 5 and 3 m electrode spacing in case of the Wenner-Schlumberger array [18]. The H1 layer was presented mainly below the field 1. It was visible especially in the transects crossing the valley thalweg (TFC5 and TFC3). The ERT transect TFT5 exhibited H1 layer only within a limited area. A key property of the H1 layer is that its shape copies the topography of the surface (compared to the H2 layer as described later). The L2 layer, which is characteristic by its comparatively low resistivity, has a variable thickness and even reaches the soil surface at the BFC3 transect. The delineation between the layers L2 and H2 is not very sharp, as compared to the divide between layers H1 and L2. This may be caused by more gradual transition between geological layers, but also by artifact of inversion, which was not successful in recognizing areas below high ρ layers (such as H1 in this case) [18] . The interface, even though not very sharp, between L2 and H2 layers clearly declines in a southern direction, the inclination does not mirror the topography of the land surface.

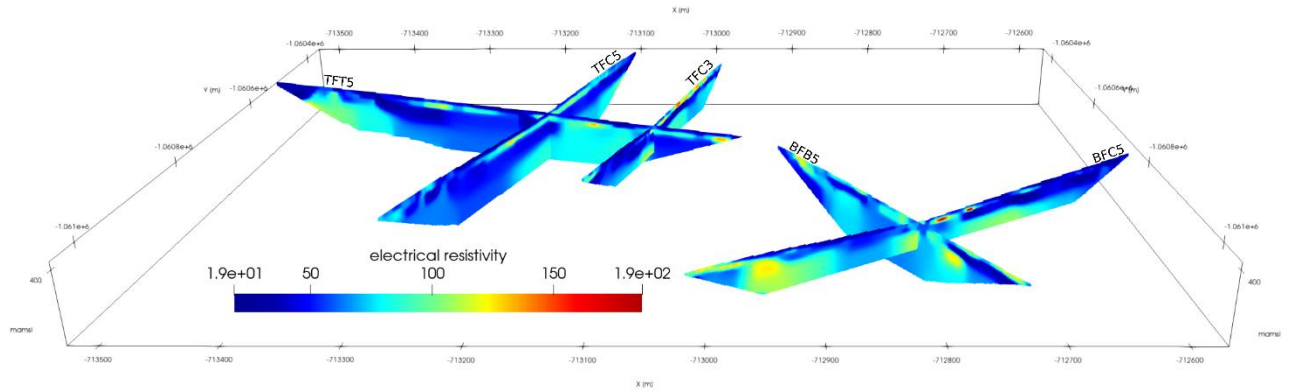

Fig. - 10. All ERT profiles shown at its real positions. Profiles coding is shown in the Figure.

The declination of the layer H2 differed for the area below field 1, and below fields 2 and 3. This difference indicates a large geological complexity in the area. At the same time, the electrical resistivity of the layers are not very different which suggest similarities within the geological layers.

The shallow and deep groundwater levels qualitatively correspond to the ERT measurements. The shallow GWL is likely positioned above the impermeable H1 layer while the deeper one above the H2 layer. The high electrical resistivity indicates rocks or less water-saturated

areas. The low electrical resistivity in layers L1 and L2 may be caused by ions dissolved in the ground water. The deep GWL derived from the borehole data was observed deeper compared to the ERT. However, the borehole was located further from the catchment in the direction of thickening of the L2 layer. It is therefore possible that the less permeable H2 layer is even deeper at the location of the borehole.

ERT transects intersections

Intersections of the ERT profiles served as cross-validation of the highly qualitative measurement which the ERT is. The transects were measured under different topsoil moisture and vegetation conditions, which may have affected the results. Also, the 2D transects which are perpendicular to each other can capture the 3D structures differently. For instance, the presence of the brook may result in differences in the transects BFB5 and BFC3 and cause the discrepancies in the intersection C [24]. The highly variable geology of the catchment and inclinations of the subsurface layers may also manifest differently to the perpendicular cross-sections. The perpendicular transects B and C exhibited larger differences. Here the differences may be also caused by different electrode spacings, where one of the transects had electrode spacing 3 and the other 5 meters. Besides these factors ERT measurement loses its sensitivity with depth and suffer various artifacts due to inversion during data processing which may also have led to deviations between profiles [25].

CONCLUSION

In this paper, we present and discuss results of a geophysical survey performed at a small headwater agricultural catchment. The survey aimed to extend the knowledge about the subsurface stratification. This information helps to interpret the water transport in the catchment and can be used for setting up the hydrological models. Results indicated a complex geology within the area. The ERT identified at least four layers with distinct electrical resistivity. Interestingly, the shallow layers (approximately 5 m below surface) corresponded to the topography of the soil surface, however, the deeper layers interface did not. These results confirm the hypothesis that portion of the water which percolates into the deep horizon can be transported from the catchment through the flow paths which do not correspond to the drainage paths inferred from the digital elevation model. Also, the shape and declination of the deep layers are different in the upper and bottom parts of the catchment which indicates heterogeneous geological setting even in a relatively small area. Although the indirect ERT method is hard to interpret quantitatively, the information presented in the manuscript increase understanding of the water transport regime within the catchment.

ACKNOWLEDGEMENTS

We would like to thank Nina Noreika, Tailin Li, Tomáš Laburda and Jáchym Jeřábek for an assistance during the labor-intensive field surveys and to Saunak Sinha Ray for the proofreading. The field work, data analysis, and manuscript preparation were funded by the Horizon 2020 research and innovation program project 773903 - “Shui - Soil Hydrology research platform underpinning innovation to manage water scarcity in European and Chinese cropping systems,” funded by the European Union, and by the Grant Agency of the Czech Technical University in Prague project no. SGS20/157/OHK1/3T/11 - “Experimentání výzkum a modelování komplexních fyzikálních procesů v půdním prostředí”.

REFERENCES

[1] Beven, K. 2006. Searching for the Holy Grail of scientific hydrology: Q_t=(S, R, Δt)A as closure. Hydrology and Earth System Sciences. Vol. 10, No. 5, p. 609–618. DOI 10.5194/hess-10-609-2006.

[2] Schrott, L., Sass, O. 2008. Application of field geophysics in geomorphology: Advances and limitations exemplified by case studies. Geomorphology. Vol. 93, No. 1–2, p. 55–73.

DOI 10.1016/j.geomorph.2006.12.024.
[3] Samouëlian, A., Cousin, I., Tabbagh, A., Bruand, A., Samouëlian, A., Cousin, I., Tabbagh, A., Bruand, A., Electrical, G.R. 2006. Electrical resistivity survey in soil science : a review . To cite this version : HAL Id : hal-00023493. .
[4] Colangelo, G., Lapenna, V., Loperte, A., Perrone, A., Telesca, L. 2008. 2D electrical resistivity tomographies for investigating recent activation landslides in Basilicata Region (Southern Italy). Annals of Geophysics. Vol. 51, No. 1, p. 275–285. DOI 10.4401/ag-3048. ze se pouziva na landslide
[5] Abudeif, A.M. 2015. Integrated electrical tomography and hydro-chemical analysis for environmental assessment of El-Dair waste disposal site, west of Sohag city, Egypt. Environmental Earth Sciences. Vol. 74, No. 7, p. 5859–5874. DOI 10.1007/s12665-015-4610-5.
[6] Wang, T.P., Chen, C.C., Tong, L.T., Chang, P.Y., Chen, Y.C., Dong, T.H., Liu, H.C., Lin, C.P., Yang, K.H., Ho, C.J., Cheng, S.N. 2015. Applying FDEM, ERT and GPR at a site with soil contamination: A case study. Journal of Applied Geophysics. Vol. 121, p. 21–30. DOI 10.1016/j.jappgeo.2015.07.005.
[7] Audebert, M., Clément, R., Moreau, S., Duquennoi, C., Loisel, S., Touze-Foltz, N. 2016. Understanding leachate flow in municipal solid waste landfills by combining time-lapse ERT and subsurface flow modelling – Part I: Analysis of infiltration shape on two different waste deposit cells. Waste Management. Vol. 55, p. 165–175. DOI 10.1016/j.wasman.2016.04.006.
[8] Sherif, M., Mahmoudi, A. El, Garamoon, H., Kacimov, A., Akram, S., Ebraheem, A., Shetty, A. 2006. Geoelectrical and hydrogeochemical studies for delineating seawater intrusion in the outlet of Wadi Ham, UAE. Environmental Geology. Vol. 49, No. 4, p. 536–551. DOI 10.1007/s00254-005-0081-4.
[9] Satriani, A., Loperte, A., Imbrenda, V., Lapenna, V. 2012. Geoelectrical surveys for characterization of the coastal saltwater intrusion in metapontum forest reserve (Southern Italy). International Journal of Geophysics. Vol. 2012. DOI 10.1155/2012/238478.
[10] Chambers, JE , Wilkinson, PB , Uhlemann, S , Sorensen, JPR , Roberts, C , Newell, AJ , Ward, WOC , Binley, Andrew , Williams, PJ , Gooddy, DC, O. 2014. Derivation of lowland riparian wetland deposit architecture using geophysical image analysis and interface detection. Water Resources Research. DOI 10.1111/j.1752-1688.1969.tb04897.x. ze se pomic ert pokouseli rozdelit jednotlive vrstby (ne jen bedrock a soil profile)
[11] Jeřábek, J., Zumr, D., Dostál, T. 2017. Identifying the plough pan position on cultivated soils by measurements of electrical resistivity and penetration resistance. Soil and Tillage Research. Vol. 174, p. 231–240. DOI 10.1016/j.still.2017.07.008.
[12] Besson, A., Cousin, I., Samouëlian, A., Boizard, H., Richard, G. 2004. Structural heterogeneity of the soil tilled layer as characterized by 2D electrical resistivity surveying. Soil and Tillage Research. Vol. 79, No. 2 SPEC.ISS., p. 239–249. DOI 10.1016/j.still.2004.07.012.
[13] Haskins, N. 2010. Book Review - A Field Guide to Geophysics in Archaeology. Archaeological Prospection. Vol. 62, No. December 2009, p. 61–62. DOI 10.1002/arp.
[14] Zhou, W., Beck, B.F., Stephenson, J.B. 2000. Reliability of dipole-dipole electrical resistivity tomography for defining depth to bedrock in covered karst terranes. Environmental Geology. Vol. 39, No. 7, p. 760–766. DOI 10.1007/s002540050491.
[15] Cheng, Q., Tao, M., Chen, X., Binley, A. 2019. Evaluation of electrical resistivity tomography (ERT) for mapping the soil–rock interface in karstic environments. Environmental Earth Sciences. Vol. 78, No. 15, p. 1–14. DOI 10.1007/s12665-019-8440-8.
[16] Noreika, N., Li, T., Zumr, D., Krasa, J., Dostal, T., Srinivasan, R. 2020. Farm-scale biofuel crop adoption and its effects on in-basin water balance. Sustainability (Switzerland). Vol. 12, No. 24, p. 1–15. DOI 10.3390/su122410596.
[17] Li, T., Jeřábek, J., Noreika, N., Dostál, T., Zumr, D. 2021. An overview of hydrometeorological datasets from a small agricultural catchment (Nučice) in the Czech Republic. Hydrological Processes. DOI 10.1002/hyp.14042.
[18] Loke, M.H. 1999. Electrical imaging surveys for environmental and engineering studies. A practical guide to 2-D and 3-D surveys. . No. 1999, p. 59.
[19] Samouëlian, A., Cousin, I., Tabbagh, A., Bruand, A., Richard, G. 2005. Electrical resistivity survey in soil science: A review. Soil and Tillage Research. Vol. 83, No. 2, p. 173–193. DOI 10.1016/j.still.2004.10.004.
[20] Palacky, G.J. 3. Resistivity Characteristics of Geologic Targets. In : Electromagnetic Methods in Applied Geophysics. 1988. p. 52–129.
[21] Furman, A., Ferré, T.P.A., Warrick, A.W. 2003. A Sensitivity Analysis of Electrical Resistivity Tomography Array Types Using. Vadose Zone Journal. Vol. 2, p. 416–423.
[22] Loke, M.H. 1998. “Res2dInv.” Rapid 2D resistivity and IP inversion using the least-squares method.

User Manual, Austin Tex, Advanced Geoscience Inc.
[23] Archie, G.E. 1942. The electrical resistivity log as an aid in determining some reservoir characteristics. Transactions of the AIME. Vol. 146, No. 01, p. 54–62.
[24] Hung, Y.C., Lin, C.P., Lee, C.T., Weng, K.W. 2019. 3D and boundary effects on 2D electrical resistivity tomography. Applied Sciences (Switzerland). Vol. 9, No. 15. DOI 10.3390/app9152963.
[25] Loke, M.H. 2004. Tutorial: 2-d and 3-d electrical imaging surveys, Geotomo Software, Malaysia. . No. July, p. 136.